



Cite this: DOI: 10.1039/d0cc06787c

Received 11th October 2020,
Accepted 2nd November 2020

DOI: 10.1039/d0cc06787c

rsc.li/chemcomm

Continuous flow synthesis of arylhydrazines via nickel/photoredox coupling of *tert*-butyl carbazate with aryl halides†

Alejandro Mata,^{ab} Duc N. Tran,^{id c} Ulrich Weigl,^d Jason D. Williams^{id *ab} and C. Oliver Kappe^{id *ab}

Nickel/photoredox catalyzed C–N couplings of hydrazine-derived nucleophiles provide a powerful alternative to Pd-catalyzed methods. This continuous-flow photochemical protocol, optimized using design of experiments, achieves these couplings in short residence times, with high selectivity. A range of (hetero)aryl bromides and chlorides are compatible and understanding of process stability/reactor fouling has been discerned.

Since its development over the past 20 years the Buchwald–Hartwig coupling, which facilitates the coupling of aryl halides with nitrogen nucleophiles, is now a staple organic transformation.¹ An important sub-group of these cross couplings involves the use of hydrazine and hydrazine-derived nucleophiles. The resulting arylhydrazines are useful intermediates in numerous heterocycle-forming reactions, or as onward nucleophiles in their own right.

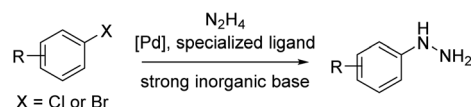
Palladium-catalyzed cross-couplings of hydrazine² and its derivatives³ have also been a focus of research, but generally requires the use of specialized phosphine ligands, and an inorganic base (Scheme 1a). Additional applications of these Pd-catalyzed protocols include aqueous micellar catalysis, with a low Pd loading,⁴ and an example conducted in flow, with short residence time and low temperature.⁵ Similarly, nickel-catalyzed methods have seen significant recent attention, but also necessitate specific ligands and inorganic bases.⁶

The application of nickel/photoredox dual catalysis has, since its introduction in 2016,⁷ become a commonly studied alternative for classical palladium- and nickel-catalyzed Buchwald–Hartwig

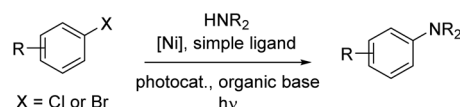
couplings in general (Scheme 1b).⁸ This is owing to the use of cheaper (often bipyridyl-based) ligands and weaker amine bases. These couplings have benefitted from the development of protocols using a range of photocatalysts⁹ and nitrogen nucleophiles.¹⁰ The relatively high reaction efficiencies, rates, and lack of complex ligands has driven the adaptation to continuous flow processes,¹¹ including demonstrations on industrially-relevant scale.¹²

Despite the growing interest in developing these photochemical dual catalytic methodologies there are, to our knowledge, no published examples involving hydrazine-derived nucleophiles.¹³ These nucleophiles represent electronically very different species, compared to other *N*-nucleophiles studied in photochemical coupling reactions. This is expected to have a particularly marked

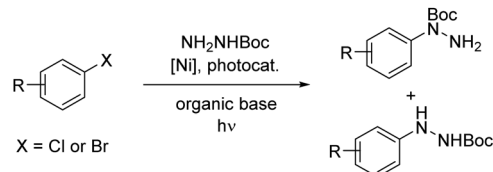
a) Pd-catalyzed couplings of hydrazine derivatives



b) Nickel/photoredox C–N couplings



c) This work: Nickel/photoredox *N*-Boc hydrazine coupling in flow



Scheme 1 (a) Literature precedents of Pd-catalyzed couplings of hydrazine derivatives with aryl halides. (b) Literature precedents of nickel/photoredox catalyzed couplings of amines with aryl halides. (c) This work: nickel/photoredox catalyzed couplings of *tert*-butyl carbazate with aryl halides to form arylhydrazine derivatives.

^a Center for Continuous Flow Synthesis and Processing (CC FLOW), Research Center Pharmaceutical Engineering GmbH (RCPE), Inffeldgasse 13, 8010 Graz, Austria. E-mail: jason.williams@rcpe.at, oliver.kappe@uni-graz.at; Web: <http://goflow.at>

^b Institute of Chemistry, University of Graz, NAWI Graz, Heinrichstrasse 28, 8010 Graz, Austria

^c Janssen Pharmaceutica N.V., Turnhoutseweg 30, 2340 Beerse, Belgium

^d Cilag AG, Hochstrasse 201, 8200 Schaffhausen, Switzerland

† Electronic supplementary information (ESI) available. See DOI: 10.1039/d0cc06787c

impact, since the amine is often proposed to also act as a ligand for nickel in these coupling procedures.^{9a} Based on our interest in synthetic organic photochemistry enhanced by improved performance and scalability bestowed by continuous flow processing,¹⁴ we endeavored to fulfill this unmet need (Scheme 1c).

As a model reaction, 4-bromo trifluorotoluene **1** was used as the aryl halide coupling partner, to allow straightforward reaction analysis by ¹⁹F NMR. The initial batch optimization efforts targeted hydrazine hydrate as the nucleophile, however, these experiments resulted in complete selectivity for dehalogenation of the aryl halide coupling partner, with no coupling observed in any case (see ESI,† Table S2). This was even observed to be the case in the absence of photocatalyst, with irradiation at 365 nm, likely due to the formation of a nickel-hydrazine complex, which absorbs at short wavelengths.^{9c}

Upon changing the hydrazine derivative to *tert*-butyl carbamate (NH₂NHBoc), a more promising outcome was achieved. It was observed that two isomers of the desired product were formed (**2a** and **2b**), alongside the dehalogenation product **1b** (Table 1). An initial optimization campaign was carried out in batch, in order to determine the optimal catalyst system and solvent (see ESI,† Tables S3–S5). Interestingly, it was observed that the photocatalyst [Ir(dtbbpy)(ppy)₂](PF₆) was far superior to the usually employed [Ir(dF(CF₃)ppy)₂(dtbbpy)]PF₆.^{7,12a} Furthermore, DMSO appeared to be far superior to other solvents and a ligand-free protocol was found to be most appropriate.

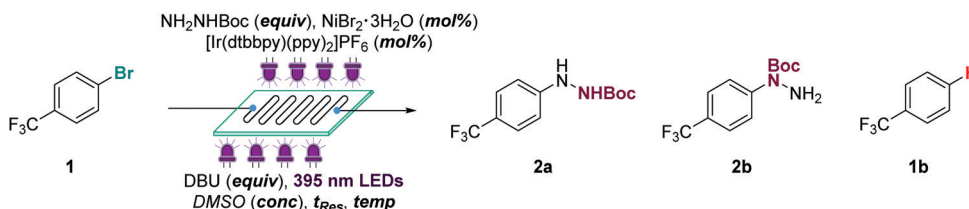
Flow experiments were carried out using a glass Corning Advanced-Flow Lab Photo Reactor,¹⁵ which facilitates high light flux at a range of different LED wavelengths. Furthermore, the integration of a heat exchange channel allows processing at

high temperatures. Finally, the reactor has been developed with scalability in mind, meaning that the methodology developed here should be scalable to larger versions of this photoreactor (*i.e.* G1 and G3).¹⁶

Optimization in flow began with irradiation at 450 nm, where only 27% of the starting aryl halide **1** was consumed (entry 1). A comparison of irradiation wavelengths revealed 395 nm to be favorable (entry 2), likely due to the higher absorption by the photocatalyst at this shorter wavelength.¹⁷ Lowering the photocatalyst loading to 0.25 mol% significantly decreased the reaction rate (entry 3), but this was then restored by increasing the reaction temperature to 80 °C (entry 4). It should be noted that for temperatures above 40 °C, a pressure of 6 bar was applied to the reactor (using a Zaiput BPR-10 back pressure regulator), to ensure that no volatile reaction components would vaporize in the process.

Based on this initial knowledge a Design of Experiments (DoE) study was carried out for detailed optimization of the reaction conditions. To avoid complete conversion, which provides limited reaction knowledge, the study was carried out at 50% of the total light intensity and 10 min residence time. Six variables were examined: all reagent and catalyst loadings, alongside temperature and concentration. A total of 19 experiments were performed (16 corner points and 3 center points), resulting in excellent models for four measured outputs: starting material **1** (inverse of reaction conversion), product **2a**, both regioisomers **2a** + **2b**, and dehalogenation side product **1b**. Selected results from this study are presented in Table 1 (entries 5–9), but complete model details and statistics are presented in the ESI.†

Table 1 Optimization of nickel/photoredox C–N coupling in flow, including selected entries (5–9) taken from a DoE study (see ESI for full details)



Entry	NH ₂ NHBoc loading (equiv.)	Photocatalyst loading (mol%)	DBU loading (equiv.)	NiBr ₂ ·3H ₂ O loading (mol%)	Conc. (M)	Residence time (min)	Temp. (°C)	1 [%] ^a	2a [%] ^a	2b [%] ^a	1b [%] ^a
1 ^b	3	0.5	2	5	0.2	20	40	73	20	3	3
2	3	0.5	2	5	0.2	20	40	65	25	5	5
3	3	0.25	2	5	0.2	20	40	76	18	2	4
4	3	0.25	2	5	0.2	20	80	16	64	12	7
5 ^c	3	0.3	2.25	5	0.3	10	100	72	22	1	5
6 ^c	2	0.1	1.5	2.5	0.4	10	120	79	16	1	4
7 ^c	2	0.5	1.5	7.5	0.4	10	80	83	14	1	2
8 ^c	4	0.1	3	2.5	0.2	10	120	76	18	1	5
9 ^c	2	0.5	1.5	7.5	0.2	10	120	32	56	2	9
10	2	0.5	1.2	7.5	0.2	10	120	<1	84	8	8
11 ^d	2	0.5	1.2	7.5	0.2	10	120	99	<1	<1	1
12 ^e	3	0.5	2	5	0.2	—	35	<1	82	10	8

^a Product ratios were determined by ¹⁹F NMR analysis. ^b Reaction was irradiated at 450 nm. ^c Reaction was run as part of a DoE study, using only 50% light intensity, to prevent complete conversion from being reached. ^d Reaction was performed in the absence of light. ^e Reaction was run in batch, using 450 nm LEDs with 20 h reaction time.

The key findings from this study show that the reaction rate is strongly dependent on high photocatalyst loading (likely due to the short path length provided by this reactor) and high temperature. Conversely to related protocols,^{9b,11a} faster reaction was observed with lower concentration. Loading of nickel catalyst, *tert*-butyl carbazate and DBU had only minor influences. These parameter dependencies, and the requirement for a highly reducing photocatalyst, suggest that the reaction mechanism may involve the reduction of the aryl halide by the photocatalyst, rather than direct oxidative addition by the nickel catalyst, as proposed for similar transformations.¹⁸

Based on these findings, a set of reaction conditions were selected, which provided complete conversion in 10 min residence time, with only 8% of the dehalogenation side product **1b** (entry 10). To ensure that this reaction is not progressing thermally, a control reaction was performed without light (entry 11), which showed minimal dehalogenation and none of the desired coupling products. A comparison with batch conditions is shown (entry 12), which provided similar results, but highlights the intensification achieved in flow, by a significant reduction in reaction time.

Using these conditions, a substrate scope was carried out, to determine the applicability of this method to other aryl halides (Scheme 2). Since both *N*-coupled regioisomers were expected, the mixture of products was subjected to Boc deprotection (4 M HCl in dioxane), to furnish a single arylhydrazine product as

the HCl salt. The model substrate **1** reacted with good selectivity and its corresponding HCl salt was isolated in 86% yield, in congruence with the optimization experiments (Table 1, entry 10).

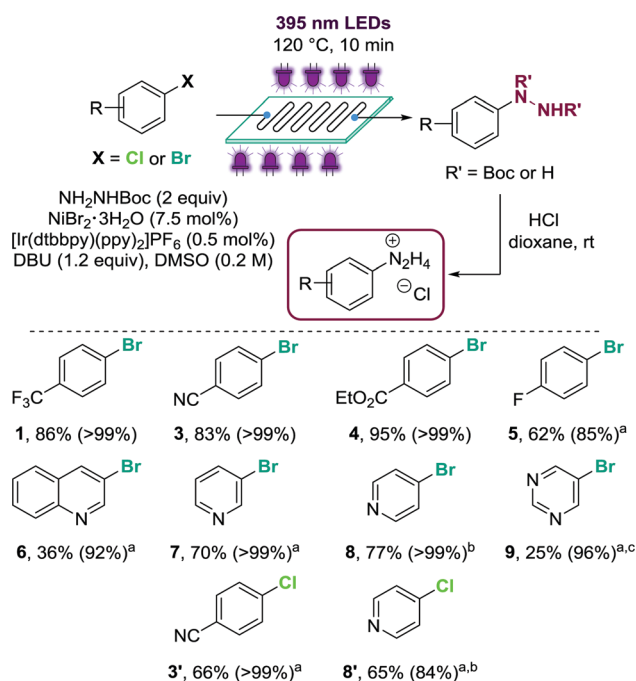
Other electron-poor aryl bromides (**3** and **4**) showed excellent reactivity, furnishing their products in high yields (83% and 95%, respectively). The more challenging *p*-fluoro substrate **5**^{9b} required a longer residence time of 20 min to reach a high level of conversion, providing a moderate yield. Electron-neutral *m*-bromotoluene reached only relatively low levels of conversion (58%, see ESI†), even at 20 min residence time. Electron-neutral and -rich substrates are known to be challenging for these methodologies^{9a} and would likely require reoptimization to achieve synthetically useful results.

Our attention then turned toward *N*-heterocyclic substrates, where almost complete conversion was achieved in the photocatalytic step, despite most substrates (**6**, **7** and **9**) requiring a 20 min residence time. Good yields were achieved for pyridine substrates **7** and **8**, whilst pyrimidine substrate **9** was isolated as the Boc protected intermediate in relatively low yield, due to instability of the hydrazine HCl salt. Finally, it was envisaged that this procedure could also be applied to more challenging aryl chloride substrates. Gratifyingly, it was found that substrates **3'** and **8'** underwent good conversion in the photochemical step, allowing isolation of the corresponding arylhydrazine HCl salts in 66% and 65% yields, respectively.

A selection of other aryl halide substrates were found to be incompatible with these reaction conditions – most markedly, *ortho*-substituted aryl bromides showed almost no reactivity. This is proposed to be due to the dramatic steric effect on the nickel catalytic cycle. Furthermore, expanding this procedure to other hydrazine derivatives (*e.g.* methylhydrazine and phenylhydrazine) showed no significant quantity of the coupling product, only dehalogenation of the aryl halide substrate (see ESI† for details of unsuccessful substrates).

In order to further capitalize on the benefits of flow processing for photochemical transformations, a scale-out experiment using the model substrate was attempted (Fig. 1). This involved processing 100 mL of starting material solution (340 min processing time), using the previously optimized conditions. In this case, after 80 min, the reaction yield began to decrease gradually, ending in only 73% conversion at the end of the process (Fig. 1b). This was found to be due to the formation of Ni(0) on the inside of the reactor, which blocks the incident light, hindering reaction progress (see ESI† for a photograph of the fouled reactor).

Based on previously published mechanistic work,¹⁸ it was proposed that the extent of Ni(0) formation could be limited by reducing the loading of photocatalyst. However, from the previous DoE studies, it is clear that this would decrease the rate of reaction. As a compromise, a lower photocatalyst loading (0.25 mol% instead of 0.5 mol%) was paired with a longer residence time (20 min instead of 10 min). The reaction was run for the same length of time and the level of conversion was maintained ($\geq 99\%$) for 260 min, decreasing to 93% after 340 min (Fig. 1c).



Scheme 2 Substrate scope of aryl halides using the developed reaction conditions in flow, followed by Boc deprotection in batch. Yields shown are that of isolated HCl salt products ($2 \times \text{HCl}$ for *N*-heterocycles). Value in parentheses denotes the conversion of starting material, as observed by HPLC (vs. internal standard) in the photochemical step. ^aReaction was performed using a 20 min residence time. ^bStarting material was used as the HCl salt, so an additional equivalent of DBU was added to the reaction mixture. ^cProduct was isolated as the Boc protected intermediate.

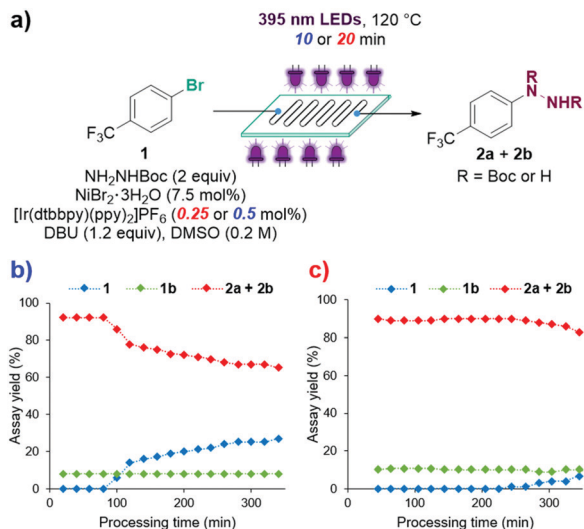


Fig. 1 Scale-out processing of the developed protocol. Assay yields were determined by ¹⁹F NMR integration. (a) Reaction conditions used. (b) Product profile over time, using conditions in blue (high photocatalyst loading, short residence time). (c) Product profile over time, using conditions in red (low photocatalyst loading, long residence time).

In summary, we present the first nickel/photoredox methodology for the formation of arylhydrazine derivatives. This methodology was rapidly optimized in continuous flow, using a combination of one factor at a time and DoE experiments, providing an in-depth understanding of the influence of each reaction variable. The optimized conditions were found to be applicable to a range of aryl halide substrates, including N-heterocycles and some aryl chlorides. Finally, a scale-out experiment demonstrated the issues of Ni(0) formation over time, but this could be minimized using altered reaction conditions for more stable processing.

Conflicts of interest

There are no conflicts to declare.

Notes and references

- (a) P. Ruiz-Castillo and S. L. Buchwald, *Chem. Rev.*, 2016, **116**, 12564–12649; (b) J. Bariwal and E. Van Der Eycken, *Chem. Soc. Rev.*, 2013, **42**, 9283–9303.
- (a) R. J. Lundgren and M. Stradiotto, *Angew. Chem., Int. Ed.*, 2010, **49**, 8686–8690; (b) J. Y. Wang, K. Choi, S. J. Zuend, K. Borate, H. Shinde, R. Goetz and J. F. Hartwig, *Angew. Chem., Int. Ed.*, DOI: 10.1002/anie.202011161.
- (a) S. Cacchi, G. Fabrizi, A. Goggiamani and S. Sgalla, *Adv. Synth. Catal.*, 2007, **349**, 453–458; (b) A. Reichelt, J. R. Falsey, R. M. Rzasa, O. R. Thiel, M. M. Achmatowicz, R. D. Larsen and D. Zhang, *Org. Lett.*, 2010, **12**, 792–795; (c) S. Cacchi, G. Fabrizi, A. Goggiamani, E. Licandro, S. Maiorana and D. Perdicchia, *Org. Lett.*, 2005, **7**, 1497–1500; (d) F. F. Ma, Z. Y. Peng, W. F. Li, X. M. Xie and Z. Zhang, *Synlett*, 2011, 2555–2558; (e) Z. Wang, R. T. Skerlj and G. J. Bridger, *Tetrahedron Lett.*, 1999, **40**, 3543–3546.

- E. B. Landstrom, N. Akporji, N. R. Lee, C. M. Gabriel, F. C. Braga and B. H. Lipshutz, *Org. Lett.*, 2020, **22**, 6543–6546.
- A. DeAngelis, D. H. Wang and S. L. Buchwald, *Angew. Chem., Int. Ed.*, 2013, **52**, 3434–3437.
- For selected examples, see: (a) R. T. McGuire, C. M. Simon, A. A. Yadav, M. J. Ferguson and M. Stradiotto, *Angew. Chem., Int. Ed.*, 2020, **59**, 8952–8956; (b) A. V. Gatién, C. M. Lavoie, R. N. Bennett, M. J. Ferguson, R. McDonald, E. R. Johnson, A. W. H. Speed and M. Stradiotto, *ACS Catal.*, 2018, **8**, 5328–5339; (c) R. T. McGuire, J. F. J. Paffile, Y. Zhou and M. Stradiotto, *ACS Catal.*, 2019, **9**, 9292–9297; (d) J. P. Tassone, E. V. England, P. M. MacQueen, M. J. Ferguson and M. Stradiotto, *Angew. Chem., Int. Ed.*, 2019, **58**, 2485–2489.
- E. B. Corcoran, M. T. Pirnot, S. Lin, S. D. Dreher, D. A. Dirocco, I. W. Davies, S. L. Buchwald and D. W. C. Macmillan, *Science*, 2016, **353**, 279–283.
- C. Cavedon, P. H. Seeberger and B. Pieber, *Eur. J. Org. Chem.*, 2020, 1379–1392.
- For selected examples, see: (a) M. Kudisch, C.-H. Lim, P. Thordarson and G. M. Miyake, *J. Am. Chem. Soc.*, 2019, **141**, 19479–19486; (b) S. Gisbertz, S. Reischauer and B. Pieber, *Nat. Catal.*, 2020, **3**, 611–620; (c) C. H. Lim, M. Kudisch, B. Liu and G. M. Miyake, *J. Am. Chem. Soc.*, 2018, **140**, 7667–7673; (d) Y. Y. Liu, D. Liang, L. Q. Lu and W. J. Xiao, *Chem. Commun.*, 2019, **55**, 4853–4856; (e) J. A. Caputo, L. C. Frenette, N. Zhao, K. L. Sowers, T. D. Krauss and D. J. Weix, *J. Am. Chem. Soc.*, 2017, **139**, 4250–4253.
- A. Wimmer and B. König, *Org. Lett.*, 2019, **21**, 2740–2744.
- (a) B. Y. Park, M. T. Pirnot and S. L. Buchwald, *J. Org. Chem.*, 2020, **85**, 3234–3244; (b) C. Rosso, S. Gisbertz, J. D. Williams, H. Gemoets, W. Debrouwer, B. Pieber and C. O. Kappe, *React. Chem. Eng.*, 2020, **5**, 597–604.
- (a) K. C. Harper, E. G. Moschetta, S. V. Bordawekar and S. J. Wittenberger, *ACS Cent. Sci.*, 2019, **5**, 109–115; (b) E. B. Corcoran, J. P. McMullen, F. Lévesque, M. K. Wismer and J. R. Naber, *Angew. Chem., Int. Ed.*, 2020, **59**, 11964–11968.
- Photochemical examples are not known, but for intramolecular Ni-catalyzed hydrazine couplings: C. Wiethan, C. M. Lavoie, A. Borzenko, J. S. K. Clark, H. G. Bonacorso and M. Stradiotto, *Org. Biomol. Chem.*, 2017, **15**, 5062–5069.
- For selected reviews of flow photochemistry, see: (a) D. Cambié, C. Bottecchia, N. J. W. Straathof, V. Hessel and T. Noël, *Chem. Rev.*, 2016, **116**, 10276–10341; (b) M. B. Plutschack, B. Pieber, K. Gilmore and P. H. Seeberger, *Chem. Rev.*, 2017, **117**, 11796–11893; (c) J. D. Williams and C. O. Kappe, *Curr. Opin. Green Sustainable Chem.*, 2020, **25**, 100351; (d) F. Politano and G. Oksdath-Mansilla, *Org. Process Res. Dev.*, 2018, **22**, 1045–1062; (e) J. P. Knowles, L. D. Elliott and K. I. Booker-Milburn, *Beilstein J. Org. Chem.*, 2012, **8**, 2025–2052.
- For selected examples of flow photochemistry performed using the same reactor, see: (a) C. Rosso, J. D. Williams, G. Filippini, M. Prato and C. O. Kappe, *Org. Lett.*, 2019, **21**, 5341–5345; (b) A. Steiner, J. D. Williams, O. de Frutos, J. A. Rincón, C. Mateos and C. O. Kappe, *Green Chem.*, 2020, **22**, 448–454.
- For selected examples of chemistry in Corning G1 and G3 photo-reactors, see: (a) P. Bianchi, G. Petit and J.-C. M. Monbaliu, *React. Chem. Eng.*, 2020, **5**, 1224–1236; (b) J. D. Williams, M. Nakano, R. Gérardy, J. A. Rincon, O. de Frutos, C. Mateos, J.-C. M. Monbaliu and C. O. Kappe, *Org. Process Res. Dev.*, 2019, **23**, 78–87; (c) A. Steiner, P. M. C. Roth, F. Strauß, G. Gauron, G. Tekautz, M. Winter, J. D. Williams and C. O. Kappe, *Org. Process Res. Dev.*, 2020, **24**, 2208–2216.
- D. Tordera, M. Delgado, E. Ortí, H. J. Bolink, J. Frey, M. K. Nazeeruddin and E. Baranoff, *Chem. Mater.*, 2012, **24**, 1896–1903.
- J. A. Malik, A. Madani, B. Pieber and P. H. Seeberger, *J. Am. Chem. Soc.*, 2020, **142**, 11042–11049.